

# Monte-Carlo calculation of the lateral Casimir forces between rectangular gratings within the formalism of lattice quantum field theory

Oleg Pavlovsky,<sup>†</sup> Maxim Ulybyshev<sup>‡</sup>

*Institute for Theoretical Problems of Microphysics,  
Moscow State University*

<sup>†</sup> *E-mail: ovp@goa.bog.msu.ru* <sup>‡</sup> *E-mail: ulybyshev@goa.bog.msu.ru*

## Abstract

We propose a new Monte-Carlo method for calculation of the Casimir forces. Our method is based on the formalism of noncompact lattice quantum electrodynamics. This approach has been tested in the simplest case of two ideal conducting planes. After this the method has been applied to the calculation of the lateral Casimir forces between two ideal conducting rectangular gratings. We compare our calculations with the results of PFA and “Optimal” PFA methods.

Key words: Lattice gauge theory, Quantum electrodynamics, Casimir effect.

PACS numbers: 11.15.Ha, 12.20.Ds.

## Introduction

The Casimir effect attracts significant attention in the last few years due to its important role in micro- and nano- mechanics [1]. There are two main problems in this area: calculation of Casimir forces for bodies that are interesting from experimental point of view; consideration of both the complicated shape and electromagnetic properties of the interacting bodies. It is also important to take into account temperature effects. Radiative corrections are small in QED [2]. But they may play more important role in case of non-abelian fields. Our approach makes it possible to take them into account.

There are many numerical methods have been proposed for calculation of the Casimir energy. Let us discuss some of them.

One of the most efficient methods for Casimir energy calculation was derived in [3]. In this case the stress tensor and the net force on a body is obtained from Euclidean Green’s function. It can be calculated numerically by using of standard electromagnetic methods (for example, by Finite Elements Method or Boundary Elements Method).

Another interesting numerical method for the Casimir energy calculation was proposed in [4]. This worldline algorithm is formulated for calculations of Casimir forces induced by scalar-field fluctuations with Dirichlet boundary conditions for various geometries. Unfortunately this method was not extended to Neumann boundary conditions.

Our approach is based on Quantum Field Theory on the lattice. It is one of the common frameworks in modern science. It is based on the Monte-Carlo calculations and provides an efficient tool to study all the above-mentioned problems. We have already studied the Casimir interaction of the Chern-Simons surfaces by using lattice QED [5, 6]. In the present paper we consider Monte-Carlo calculation of the Casimir interaction between ideal conductors and between dielectric bodies. As an example, we study the Casimir effect for two rectangular

gratings. The normal part of the vacuum force in this system has already been calculated [7]. But there exist also lateral forces, which are of significant experimental and technical interest.

# 1 Ideal conductors and dielectric bodies in QED on the lattice

## 1.1 Conductor boundary conditions

In this paper we use the 4-dimensional hypercubical lattice and the simplest action of noncompact lattice QED in Euclidean time:

$$S = \frac{\beta}{2} \sum_x \sum_{\mu < \nu} \theta_{\mu\nu}^2(x), \quad (1)$$

where the link and plaquette variables are defined as follows:

$$\begin{aligned} U_\mu(x) &= e a A_\mu, \\ \theta_{\mu\nu}(x) &= \Delta_\mu U_\nu(x) - \Delta_\nu U_\mu(x), \\ \Delta_\mu U_\nu(x) &= U_\nu(x + \hat{\mu}) - U_\nu(x), \end{aligned} \quad (2)$$

where  $a$  is the lattice step,  $\beta = 1/e^2$ . The lattice is formed by the sites. They are vertices of 4-dimensional cubes. The links are edges of these cubes and plaquettes are their sides. The functional integrals for physical quantities are calculated by means of the Monte-Carlo method. It means that we generate field configurations (sets of link variables) with statistical weight  $e^{-S}$ . After it the functional integrals are calculated as field configurations averages.

Our first task is formulation of the ideal conductor boundary condition on the lattice. Both electric and magnetic fields are pushed away from the interior of conductor. So the boundary conditions for the fields can be written as:

$$E_{\parallel}|_S = 0, \quad H_n|_S = 0. \quad (3)$$

Because the hypercubical lattice is used in our approach, we will approximate a surface by a set of plane polygons. Each polygon consists of plaquettes.

Let us consider a surface that consists of one polygon (normal to the z-axis). More complicated surfaces can be treated similarly. Expressions (3) are the boundary conditions for the field strength tensor  $F_{\mu\nu}$ . Due to the connection between lattice variables and fields (2), the boundary conditions can be reformulated in terms of plaquette variables:

$$\theta_{41}(x) = 0, \quad \theta_{42}(x) = 0, \quad \theta_{12}(x) = 0. \quad (4)$$

All plaquettes in these conditions form 3-dimensional sublattice that describes the conductor surface. Pure gauge is the only type of field configuration that satisfies this conditions. It means that any link variable inside this sublattice can be written as:

$$U_i = \alpha(x + \hat{i}) - \alpha(x), \quad (5)$$

where  $\alpha(x)$  is an arbitrary function defined on the sites of 3-dimensional sublattice. This scheme is valid for any surface.

The functional integrals should be rewritten, taking into account the conductor boundary conditions. Our functional integrals must be formulated in terms of independent field variables

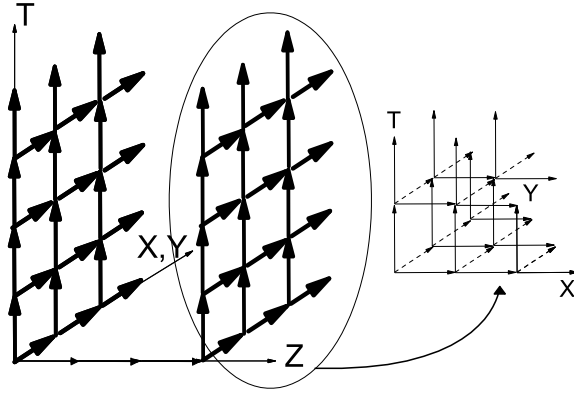


Figure 1: Two parallel conducting planes: sublattices of links with zero value link variables.

$A_\mu(x)$ , but in our case some of them are not independent due to the conditions (3). This problem can be solved by choosing the function  $\alpha(x)$  as an independent variable which parameterizes the fields on the boundary surface.

So the functional integral for the partition function takes the form:

$$Z = \int D\tilde{A}_\mu D\alpha e^{(iS[\tilde{A}_\mu, \alpha])} ,$$

where  $\tilde{A}$  is the vector potential of the fields outside the boundary surface.

Physical quantities are calculated by means of the Euclidean functional integral:

$$\langle F \rangle = \frac{\int D\tilde{A}_\mu D\alpha F[A_\mu] e^{-S_{eucl.}[\tilde{A}_\mu, \alpha]}}{\int D\tilde{A}_\mu D\alpha e^{-S_{eucl.}[\tilde{A}_\mu, \alpha]}} . \quad (6)$$

It is very important to note also that quantity  $F[A_\mu]$  is gauge invariant.

Now let us consider lattice discretization of (6). The Euclidean action  $S_{eucl.}[\tilde{A}_\mu, \alpha]$  and the observable  $F[A_\mu]$  can be rewritten in terms of lattice variables:  $S_{Eucl.Lat.}$  and  $F[U_\mu]$ . Then the functional integral is Boltzmann-type field configuration average with statistical weight  $\exp(-S)$ . The lattice field configurations consist of the link variables  $U_\mu$  and the site variables  $\alpha(x)$ . The link variables describe the electro-magnetic field outside the boundary surface. The site variables are defined on the lattice sites that belongs to boundary surface. The function  $\alpha(x)$  parameterizes the pure gauge fields on this surface.

The pure gauge field on the surface can be transformed into the zero-value fields  $\alpha(x) = 0$  by means of a suitable lattice gauge transformation. After such transformation, the action  $S_{Eucl.Lat.}$  and the observable  $F$  do not change their values. It means that in order to implement the ideal conductor boundary conditions it is sufficient to generate field configurations with zero-value link variables on the boundary surface.

Let us consider the following example: the Casimir interaction of two parallel conducting planes.

The boundary links are always taken equal to zero during the generation procedure. In Fig. 1, these boundary links are bold-marked. The boundary links form two 3-dimensional sublattices at  $z = 0$  and  $z = N$ , where  $N$  is lattice size. The 3-dimensional structure of these sublattices is shown in Fig. 1 as well. These boundary conditions can be written explicitly as

$$U_i(x, y, z, t) = 0 \quad \text{if} \quad i = 1, 2, 4 \quad \text{and} \quad z = 0, N .$$

The periodic boundary conditions are used for the other three coordinates ( $x$ ,  $y$  and  $t$ ).

This approach can be used to implement the ideal conductor boundary conditions for any surface shape.

## 1.2 Description of dielectric bodies in QED on the lattice

The simplest dielectric (we neglect anisotropy and dielectric constant frequency dependence) can be described by the following action:

$$S = \frac{1}{4} \int_{\tilde{V}} F_{\mu\nu} F^{\mu\nu} dV + \frac{1}{2} \int_V \left( \varepsilon \sum_{i=1}^3 F_{0i} F^{0i} + \sum_{i<j} F_{ij} F^{ij} \right) dV.$$

Here  $V$  is the 4-dimensional volume occupied by dielectric body and  $\varepsilon$  is the static dielectric constant. This action can be rewritten in terms of lattice quantities:

$$S = \frac{\beta}{2} \left( \sum_{x \in \tilde{V}} \sum_{\mu < \nu} \theta_{\mu\nu}^2(x) + \sum_{x \in V} \left( \varepsilon \sum_{i=1}^3 \theta_{0i}^2(x) + \sum_{i < j} \theta_{ij}^2(x) \right) \right).$$

We shall use it for field configurations generation. The dielectric constant frequency dependence is very important for real materials and has to be taken into account. Firstly, we fix the gauge:

$$A_4 = 0.$$

Then we make the Fourier transform:

$$A_i = \frac{1}{\sqrt{2\pi}} \int \tilde{A}_i e^{-i\omega\tau} d\omega, \quad i = 1, 2, 3.$$

Here  $\omega$  is the imaginary frequency, since we make the Fourier transform in Euclidean time. After this, the action becomes “block-diagonal”:

$$S_{\text{eucl}} = \frac{1}{2} \int d\vec{r} d\omega \left( \tilde{F}_{12}^2 + \tilde{F}_{13}^2 + \tilde{F}_{23}^2 + \varepsilon(i\omega)\omega^2(\tilde{A}_1^2 + \tilde{A}_2^2 + \tilde{A}_3^2) \right).$$

So we can generate field configurations for each  $\omega$  independently and take into account the  $\varepsilon(\omega)$  dependence.

## 2 The lattice observable for the ground state energy

The corresponding lattice observable should give (after the Monte-Carlo averaging) the ground state energy of a system:

$$\int_V \langle 0 | T^{00} | 0 \rangle d\vec{x}. \quad (7)$$

Our task now is to define such lattice observable.

Lattice system can be treated as a certain  $N$ -dimensional quantum-mechanical system where the number of degrees of freedom  $N$  tends to infinity. For simplicity we will firstly consider the one-dimensional problem of quantum particle moving in potential  $V(x)$ . The lattice formulation of this task: the path in functional integral is a set of the coordinate values at different moments of time ( $x(t_i) = x_i$ ,  $i = 0 \dots N$ ). The boundary conditions in the Euclidean time direction are taken periodic:  $x_0 = x_N$ . Such a path is an analog of the Euclidean field configuration in

Lattice Field Theory. The Monte-Carlo method for functional integral calculation is based on generation of a set of such lattice configurations with statistical weight proportional to  $\exp(-S_{\text{eucl}}[x]/\hbar)$ . The Euclidean action is

$$S_{\text{eucl}} = a \sum_{n=1}^N \left( \frac{m(x_n - x_{n-1})^2}{2a^2} + V(x_n) \right),$$

where  $a$  is the time step. It is well known [10] that any coordinate  $x_n$  is distributed with the probability density of the vacuum state. It means that if one calculates the configuration average of a certain lattice observable (for example, the potential energy), one gets the vacuum average of this observable (the average potential energy):

$$\langle 0|V|0 \rangle = \langle V(x_n) \rangle = \frac{1}{N_{\text{conf}}} \sum_{\text{conf}} V(x_n).$$

In order to obtain the full energy of the system, we need to calculate the average of the kinetic energy as well. This problem was studied in [9], the corresponding lattice observable for the kinetic energy is given by

$$\langle 0|T|0 \rangle = \left\langle -\frac{m}{2} \frac{(x_{n+1} - x_n)^2}{a^2} + \frac{\hbar}{2a} \right\rangle. \quad (8)$$

The naive expression for the kinetic energy lattice observable (the first part in the sum (8)) diverges in the continuous limit due to fractal structure of the trajectories. This divergence is directly cancelled in (8). This procedure can be performed for any lattice models (and for lattice field theory too), and thus we have the method for direct calculation of the full energy on the lattice.

Let us consider noncompact lattice QED with the Hamiltonian density:

$$\mathcal{H} = \frac{1}{2} \left( \sum_{i=1}^3 \pi_i(\vec{x})^2 + \sum_{i<j} F_{ij}(\vec{x})^2 \right), \quad (9)$$

where the “field momentum”  $\pi_i = F_{0i}$  is the conjugated quantity to the field  $A_i$ . The vacuum expectation value of the second part of the expression (9) can be calculated directly by the field configuration averaging. The averaging of the first part of (9) is performed by the same way as the kinetic part of one-dimensional quantum mechanical system: we calculate the same observable, but with opposite sign at  $\pi_i(\vec{x})^2$ . The final expression for vacuum expectation value of the full energy reads

$$\langle 0|H|0 \rangle = \left\langle \frac{\beta}{2} \left( \sum_{x,i} (-\theta_{4i}^2(x)) + \sum_{x,i<j} \theta_{ij}^2(x) \right) \right\rangle. \quad (10)$$

The renormalization procedure for the lattice observable (10) has three parts. Firstly, the singular contribution in (8) that corresponds to fractal structure of the trajectories has to be eliminated. So we calculate the energy density  $\langle 0|T^{00}(\vec{x})|0 \rangle$  on the free lattice and then subtract it from the energy density calculated in presence of the boundaries.

$$\langle 0|T^{00}(\vec{x})|0 \rangle_{\text{bound}} - \langle 0|T^{00}(\vec{x})|0 \rangle_{\text{free lattice}}.$$

As a result, one gets the difference between the Hamiltonian densities with and without interacting bodies. It is important to note that  $\langle 0|T^{00}(\vec{x})|0 \rangle_{\text{free lattice}}$  is just a constant.

But this is not the end of the story. Any bodies have the Casimir self-energies which are connected with their boundaries. The Casimir self-energy calculation is an important task, e.g., for the dynamical Casimir effect, but in our case this type of the Casimir energy should be eliminated because we are interested only in interaction between bodies.

Finally, we have the following three stages of the renormalization procedure:

1. Calculation of the energy density  $\langle 0|T^{00}(\vec{x})|0\rangle$  in presence of the boundary conditions (interacting bodies) and subtraction of the “fractal divergence” constant  $\langle 0|T^{00}(\vec{x})|0\rangle_{\text{free lattice}}$ .
2. Calculation of the energy density  $\langle 0|T^{00}(\vec{x})|0\rangle_{\text{self-energy}}$  for all interacting bodies individually.
3. Subtraction of this Casimir self-energy density  $\langle 0|T^{00}(\vec{x})|0\rangle_{\text{self-energy}}$  from the Casimir energy density of the interacting bodies after elimination of the “fractal divergence”. As a result, one obtains the renormalized Casimir energy density for the system of the interacting bodies.

### 3 Results of the numerical calculations

We use the standard “heat bath” method [13] for field configurations generation. Also we use the anisotropic lattice to improve the accuracy of our calculations. The anisotropic lattice formalism is similar to the one applied in [11] to study the finite temperature effects, but in the present work we deform  $z$ -direction instead of  $t$ -direction.

All link variables are connected with the field components in the usual way:

$$U_\mu = e a A_\mu, \mu = 1, 2, 4$$

except links in  $z$ -direction:

$$U_3 = \alpha e a A_3.$$

Here  $a$  is the lattice step in all directions except  $z$ ;  $\alpha a$  is the lattice step in  $z$ -direction. The action can be written as

$$S = \frac{\beta}{2} \left\{ \alpha \sum_x \sum_{\mu < \nu; \mu, \nu \neq 3} \theta_{\mu\nu}^2(x) + \frac{1}{\alpha} \sum_x \sum_\nu \theta_{3\nu}^2(x) \right\}. \quad (11)$$

The continuous limit for the new observable is different from the traditional methods used, for example, in lattice QCD. It is well known that in the continuous theory the Casimir energy (without radiative corrections) is independent of the electron charge. This property is exactly reproduced in noncompact lattice electrodynamics for the following reasons. Firstly, the phase transition is absent in this theory, thus  $\beta$  in (11) plays only the role of parameter that determines the numerical values of link variables. Therefore, if one calculates the Casimir energy in noncompact electrodynamics without fermions, the value of  $\beta$  can be chosen arbitrarily within sufficiently broad range and is defined solely by the calculation convenience.

This independence of results from  $\beta$  additionally manifests itself in the fact that Casimir calculations do not actually require any knowledge about the physical volume of the lattice and the value of lattice step  $a$ . We obtain the dimensionless energy in  $\frac{1}{a}$  units. All geometrical sizes of the considered bodies are defined in the lattice step units. Therefore, the physical value of the lattice step  $a$  fixes all sizes and real physical value of the Casimir energy.

In noncompact electrodynamics, the rotational symmetry is restored automatically at sufficiently large lattice distances (this was shown, e.g., in [12]). Therefore, the continuous limit

is only the transition  $N \rightarrow \infty$ . In other words, we should find that the correct dependence of the Casimir energy on the distance between the bodies is restored at large lattice distances.

This difference between noncompact QED and non-abelian theories can be understood from the following simple arguments. We should decrease the lattice step relatively to a typical scale of the theory to achieve the continuous limit. The Compton wavelength of glueball is such a scale in non-abelian theories. We vary the relation of the lattice step to this characteristic length by changing  $\beta$ . So we can make the lattice step small in comparison with the glueball scale. It means also that the correlation length tends to infinity in the lattice units. The situation is quite different in non-compact Abelian theory. There are no glueballs in noncompact Abelian theory without fermions in the continuous limit. The correlation length is just a lattice artifact of discretization in this theory. The scale in this theory is defined by the sizes of the interacting bodies. It means that the continuous limit in this theory is archived in the case when the sizes of the bodies (in the lattice units) become large and all the lattice sizes tend to infinity.

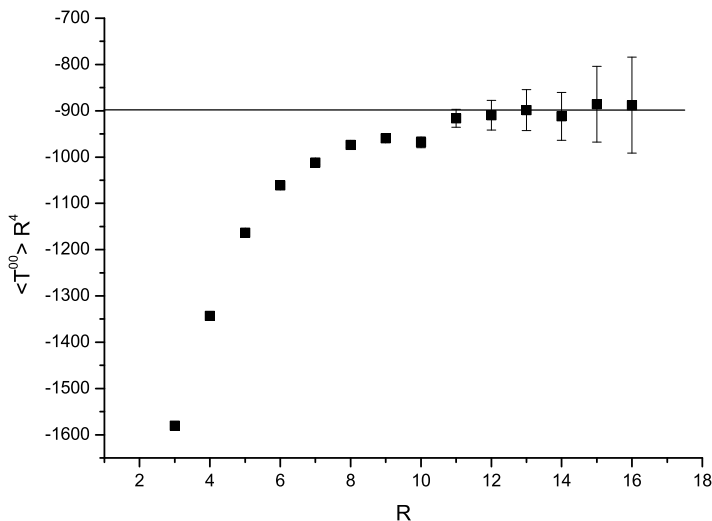


Figure 2: Calculation of  $\langle 0|T^{00}(\vec{x})|0\rangle R^4$  in case of the periodic boundary conditions,  $R$  is the size of the space region in the lattice step units. Lattice sizes:  $64 \times 64 \times 64 \times R$ . The line is the analytical answer [14].

The restoration of the continuous limit in the Casimir problem on the lattice is illustrated in Fig. 2. In this calculation the Casimir energy of the electro-magnetic field is studied in the case of the space-periodic boundary conditions. This problem provides a good test for our method because there is the analytical solution in this case [14]. The lattice observable is the vacuum energy density calculated by using the renormalization procedure which we discussed above.

The energy density of the electro-magnetic field in case of the periodic boundary conditions is a constant [14] and is proportional to  $1/R^4$ , where  $R$  is the size of the space region where we confine the fields by the periodic boundary conditions (this statement is obvious from dimensional reasons). Therefore, the quantity  $\langle 0|T^{00}(\vec{x})|0\rangle R^4$  should be constant for large size of the lattice, when the continuous limit is reproduced.

In Fig. 2 one can see that our lattice calculation of the energy density tends to the analytical result at large lattice distances  $R$ . If the lattice distance  $R$  is about 11-12 lattice units, the lattice results are very close to the analytical ones, and we can conclude that the continuous limit is achieved just at these lattice distances.

We test our method on the well-known problem of the Casimir interaction of two parallel conducting planes. In Fig. 3 the lattice calculation of the vacuum energy of the electromagnetic field is presented for this model (we study the planes with quite large size due to the continuous limit reasons). We consider two parallel planes which are separated by the distance  $D$  in  $z$ -direction. The calculations are performed on the anisotropic lattice with the following sizes:  $32a$  at  $x$ ,  $y$  and  $t$  directions,  $Ra_z$  at  $z$  direction,  $a_z/a = 1/3$ . The analytical result for this problem is well known ( $c = \hbar = 1$ ):

$$E = \frac{\pi^2 S}{720 D^3},$$

where  $S$  is the area of the planes,  $D$  is the distance between the planes. We fit the calculated points by the function  $E = P_1/R^3$  using the Least Squares method. As one can find, the dependence of the Casimir energy on the distance between planes is reproduced correctly by our lattice method. In order to compare this lattice result with the analytical answer, one should note that all geometrical sizes are proportional to the lattice step  $a$ , while the energy is proportional to  $a^{-1}$ . This means that

$$E = \frac{\pi^2 N^2}{720 \alpha^3} \frac{1}{R^3} \frac{1}{a}. \quad (12)$$

The lattice steps in  $x$ ,  $y$  and  $t$  directions are equal to  $a$ , but the lattice step is equal to  $\alpha a$  in deformed  $z$  direction. The area of the planes is equal to  $S = (Na)^2$ , where  $N$  is the lattice size in  $x$  and  $y$  directions; the distance between planes is  $D = \alpha a R$ .

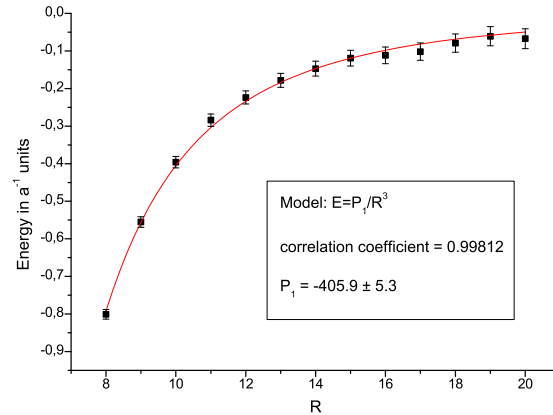


Figure 3: Calculation of the Casimir interaction energy for two parallel conducting planes.  $R$  is the distance between planes in the lattice steps:  $D = \alpha a R$ . The fitting line is found by the Least Squares method:  $y = \frac{P_1}{R^3}$ . All calculation are performed on the anisotropic lattice with the deformation coefficient  $a_z/a_{xyt} = 1/3$ . The lattice sizes:  $32a \times 32a \times 32a \times Ra_z$ .

So we have to compare the dimensionless coefficient at  $\frac{1}{R^3}$  in the expression for the Casimir energy (12) with the coefficient  $P_1$  calculated by fitting the numerical data using the function  $E = P_1/R^3$ . The analytical answer for this coefficient is  $P_1^{analyt} = 379$  (the parameters of the lattice are shown in Fig. 3). In this test problem one can find that the numerical accuracy of our approach is about 5%.

Let us apply our method to the calculation of the Casimir forces between two conducting surfaces with complicated shapes. We consider two rectangular gratings (see Fig. 4).



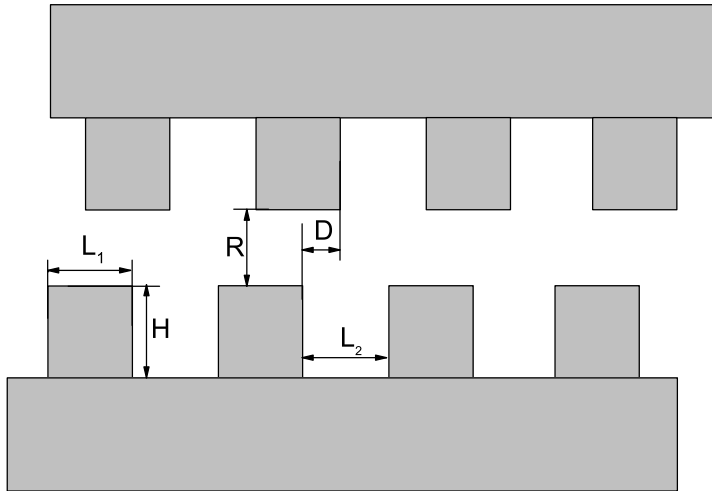


Figure 4: Geometrical parameters of the gratings.

We perform the calculation for the ideal conducting gratings with the following parameters: the width of the “tooth” and the distance between them are  $L_1 = L_2 = 7a$ ; the height of the “tooth” is  $H = 7a_z$ ; the distance between the gratings (between the tops of the “teeth”) is  $R = 8a_z$ . All sizes are chosen sufficiently large to restore the continuous limit. The lattice is the same that in the previous calculation for two planes:  $a_z/a = 1/3$ .

The result of the Casimir energy calculation for the two gratings is shown in Fig. 5.

We also compare our calculation with the results of approximate methods (PFA and “Optimal” PFA [15]). The PFA approach is often considered as the initial approximation for such systems. In the case of the two gratings interaction the PFA method yields the “saw” consisted of the straight lines. It is obvious that the deviations from the PFA are rather large, especially when the “teeth” of one grating are opposite to the wells of the other one. So a corrections to ordinary PFA should be considered. We compare our results with so-called “Optimal” PFA. It was proposed by Jaffe and Scardicchio in the paper [15]. In this approach the Casimir energy is given by:

$$E = -\frac{\pi^2}{720} \int_D d^3\vec{r} \frac{1}{(l_{12}(\vec{r}))^4}.$$

Here  $D$  is space region between the boundaries and  $l_{12}(\vec{r})$  is the shortest path that passes through the point  $\vec{r}$  from one boundary to another. Unfortunately in this case of rectangular gratings “Optimal” PFA is not fully adequate too (see Fig. 5).

We also calculate the vacuum energy density that corresponds to the gratings interaction. It is shown in Fig. 6 for different lateral shifts for Monte-Carlo calculations and for “Optimal” PFA.

The calculation of the energy density (see Fig. 6) allows us to clear up the reasons why the PFA is not appropriate for this shape of interacting surfaces. In the PFA approach, we take into account only interaction of the parts of the surfaces that lie opposite to each other. One can see in Fig. 6 that in the situation when the “teeth” are opposite to the “wells”, the vacuum energy density is concentrated in the space region between the corners of the “teeth”. And it is just the very case when the PFA gives maximal error. Hence we can conclude that the main reason for the errors in the PFA is the neglecting of those specific Casimir forces that appear

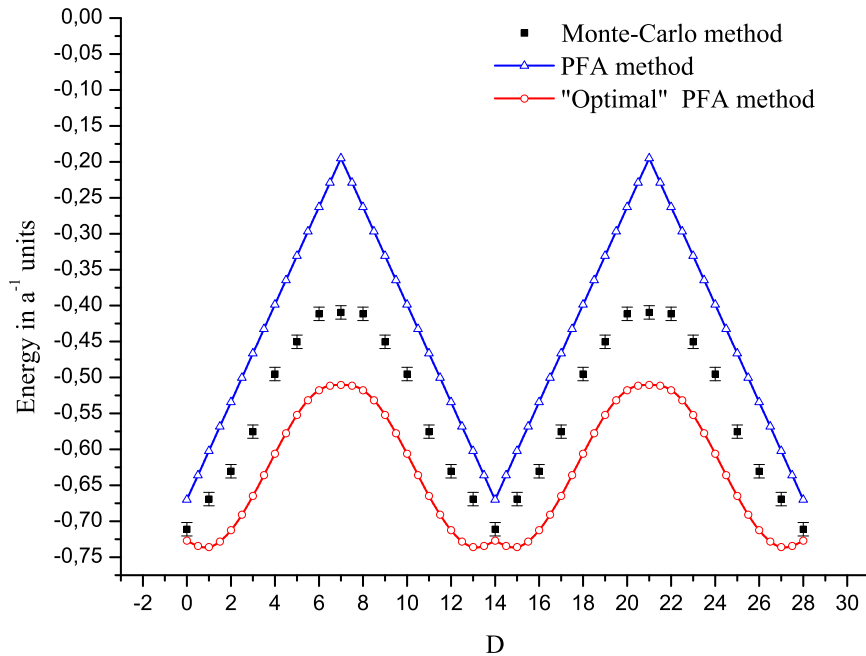


Figure 5: Vacuum energy dependence on the lateral shift of the gratings. Comparison of our Monte-Carlo calculations with the results of PFA and “Optimal” PFA methods. Lattice sizes:  $42a \times 42a \times 42a \times 22a_z$ . Deformation coefficient:  $a_z/a_{xyt} = 1/3$ .

between the “corners” of the gratings.

“Optimal” PFA takes into account the “corners” interaction. However its weak point in this geometry is the edge effect: energy density in the region between parallel parts of the gratings strongly depends on the size of this region (see the first column in Fig. 6), but in PFA and “Optimal” PFA (see the second column in Fig. 6) energy density in this region is constant.

Our method can also be considered as Monte-Carlo calculation of some elements of the Green’s function. So for abelian fields our results will be close to the results obtained by the Euclidean Green’s function method [3].

## Conclusions

We introduced the new method for calculation of the Casimir forces based on the Monte-Carlo simulations in noncompact QED on the lattice. The method consists in two parts: the definition of the boundary conditions for the field configurations; the definition of the lattice variable that gives the vacuum energy density after the averaging over these configurations.

The method is tested on the problem of the Casimir interaction of two parallel conducting plates. Also this approach is used to study the lateral Casimir forces between two rectangular gratings. The Casimir energy and the vacuum energy density for the interaction are obtained for different lateral shifts of the gratings.

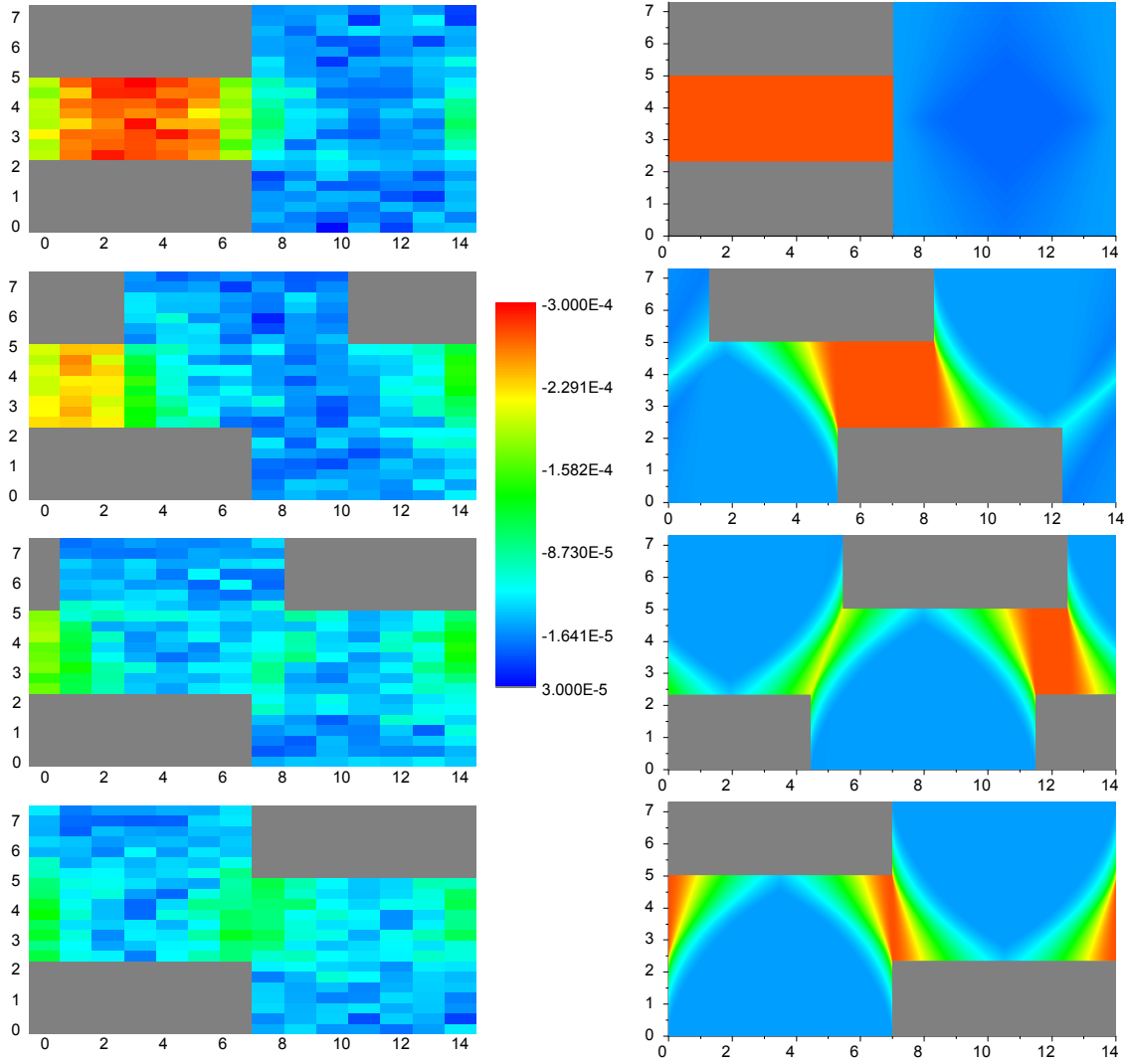


Figure 6: Vacuum energy density distribution for different lateral shifts. Results of Monte-Carlo calculations (left column) and “Optimal” PFA calculations (right column).

## Acknowledgements

The authors thank I. G. Pirozhenko and V. N. Marachevsky for the substantial discussions. Computing facilities of the MSU Supercomputer Center have been used for our calculations.

## References

- [1] M. Bordag, G. L. Klimchitskaya, U. Mohideen and V. M. Mostepanenko. *Advances in the Casimir Effect*. Oxford University Press, International Series of Monographs on Physics 145, 2009.
- [2] M. Bordag and K. Scharnhorst, *Phys. Rev. Lett.* 81 (1998) 3815.

- [3] M. T. Homer Reid, A. W. Rodriguez, J. White, and S. G. Johnson, Phys. Rev. Lett. 103 (2009) 040401; M. Levin, A. P. McCauley, A. W. Rodriguez, M. T. Homer Reid, and S. G. Johnson, Phys. Rev. Lett. 105 (2010) 090403.
- [4] H. Gies, K. Langfeld, L. Moyaerts, JHEP 018 (2003) 0306; H. Gies and K. Klingmuller, Phys. Rev. D 74 (2006) 045002.
- [5] O. Pavlovsky and M. Ulybyshev, Int. J. Mod. Phys. A 25 (2010) 2457 [arXiv:0911.2635 [hep-lat]].
- [6] O. Pavlovsky, M. Ulybyshev, Particles and Nuclei, Letters, v. 7 (2010) 483.
- [7] A. Lambrecht, V. Marachevsky, Phys. Rev. Lett. 101 (2008) 160403.
- [8] R. Buscher and T. Emig, Phys. Rev. A 69 (2004) 062101.
- [9] D. M. Ceperley, Rev. Mod. Phys. 67 (1995) 279.
- [10] M. Creutz, B. Freedman, Annals of Physics 132 (1981) 427.
- [11] G. Burgers and F. Karsch Nucl. Phys. B 304 (1988) 587.
- [12] T. A. DeGrand and D. Toussaint, Phys. Rev. D 24 (1981) 466.
- [13] Yu. Makeenko, Sov. Phys. Usp. 27 (1984) 401.
- [14] S. G. Mamayev, N. N. Trunov, Theor. Math. Phys. 38 (1979) 228.
- [15] R. L. Jaffe, A. Scardicchio, Phys. Rev. Lett. 92 (2004) 070402.